Near-monolayer ^{3}He-^{4}He films: Two superfluid transitions and the ^{3}He effective mass and binding energy

Xingwu Wang and Francis M. Gasparini
State University of New York at Buffalo, Buffalo, New York 14260
(Received 29 April 1988)

We have measured the mass loading on a torsional oscillator of mixture films of ^{3}He and ^{4}He at coverages near one active atomic layer of ^{4}He. These measurements yield information about the superfluid transition of ^{4}He and the effective mass and binding energy of ^{3}He. Unlike the situation with submonolayer and multilayer films, where the superfluid transition takes place at a single temperature, we observe for these films a transition in two steps. This confirms a report some time ago of a similar observation by Bishop and Reppy. By comparing the mass loading at $T=0$ of pure ^{4}He films with that of mixtures, we obtain the ^{3}He effective mass which can be compared with results from the specific heat. We find, in particular, that the effective mass has a maximum as a function of ^{4}He thickness with correct asymptotic values for infinite and zero thickness limits. This maximum coincides very nearly with the thickness of ^{4}He at which the transition into the superfluid state takes place in two steps. In the submonolayer region the effective mass agrees with a density dependence one might expect as an extension of the theory of Pandharipande and Itoh for three-dimensional mixtures. We believe such theory should be able to be done for the two-dimensional case.

I. INTRODUCTION

It is often believed that mixture films of ^{3}He in ^{4}He may be regarded, at their simplest, as two-dimensional analogues of three-dimensional mixtures. This view, while it contains a grain of truth, is much too simplistic and certainly does not account for a variety of experimental observations. Some of the issues which arise in the case of mixture films is the spatial configuration of the ^{3}He and ^{4}He (Refs. 1–4), the binding energy of the ^{3}He to the ^{4}He (Ref. 5); the behavior of ^{3}He as a quasi-ideal 2D Fermi gas[5,6] possible transitions involving spatial reconfiguration either along the plane of the film or orthogonal to it;[7,8] the evolution of the ^{3}He excited states from a set of 2D subbands to a 3D continuum;[2,5] and, the critical behavior of the mixture films near the superfluid transition.[4,9,10] All these issues can be explored in a thermodynamic space of temperature–^{4}He film thickness–^{3}He coverage, or perhaps more appropriately, in some limit, ^{3}He concentration. Additional questions might also arise regarding the role of the substrate, both in terms of the helium-substrate interaction, or perhaps, more subtle issues regarding the substrate topology *vis-à-vis* characteristic lengths of the helium film.[11,12]

To understand some of the above issues we might follow the evolution of a dilute submonolayer mixture of ^{3}He in superfluid ^{4}He on a planar substrate and see how this evolves upon addition of ^{4}He. Note that we concern ourselves here only with the situation where sufficient ^{4}He is present so that a superfluid film can form. This, in practice, means a fluid layer above an "inert" immobile layer of adsorbed ^{4}He (Ref. 13). This layer forms on all surfaces and is a reflection mostly on the strong helium-substrate relative to helium-helium interaction.

When the total amount of ^{3}He and superfluid ^{4}He is less than one atomic layer, one is very nearly in the two-dimensional analogue of three-dimensional mixtures.[14] Modifications may arise due to residual substrate effects being manifest near the superfluid transition mostly in the dynamics of the films, or at lower temperatures in the behavior of the ^{3}He. Contact with theories can be made in this limit. These theories yield phase diagrams similar to three-dimensional mixtures with a depression of the superfluid transition with ^{3}He and an eventual phase separation.[15–17] In experiments one does see a depression of the superfluid transition temperature, but no phase separation has been observed in this limit.[4]

When several layers of superfluid ^{4}He are present, small amounts of ^{3}He (less than one atomic layer) do not mix uniformly in the ^{4}He, but rather reside at the free surface of the film.[2] Further, experiments have shown[5] and theory supports a picture whereby the ^{3}He excited states form a set of two-dimensional subbands.[18,19] This situation is quite analogous to electrons in the inversion layer of a metal oxide semiconductor field effect transistor (MOSFETS) or in semiconductor heterostructures.[20] If one adds more ^{3}He to this film so as to saturate the surface state, some experiments indicate that a complete separation of ^{3}He and ^{4}He is retained,[3] while others suggest mixing with perhaps a phase transition into a separated phase.[4,8]

Thicker films of ^{4}He, greater than ~ 10 layers, still retain a surface state for the ^{3}He. Indeed, this is present for the surface of bulk ^{4}He where, in fact, it was first predicted to exist.[21] Small amounts of ^{3}He in a thick film of ^{4}He still act as a 2D Fermi gas at the free surface. When the surface state is saturated, or at sufficiently high temperature, the ^{3}He dissolves in the body of the film forming

now what is more and more like a slab of a three-dimensional mixture.[2,5] There is still one proviso, and that is that the ^{3}He concentration is not uniform, but rather is depleted near the substrate due to the larger local pressure from the van der Waals attraction. This effect can be calculated using properties of the 3D mixtures phase diagram.[22,23]

One can also reverse the role of ^{3}He and ^{4}He by studying a situation of a small amount of ^{4}He with a thick overlayer of ^{3}He (Refs. 4 and 24). It is interesting in this limit to study the superfluid transition of the ^{4}He bounded on both sides, as it is in this case, by a nonsuperfluid region.

In this paper we report studies of ^{3}He-^{4}He films with total thickness in the neighborhood of one atomic layer above the nonsuperfluid layer. These are measurements of the mass loading of a torsional oscillator as a probe of the superfluid transition and as a measure of the ^{3}He effective mass. There were two motivations for the start of this work. One was the observation of Bishop and Reppy that the superfluid transition in a near monolayer mixture film took place in two steps.[25] Second, was the specific heat results of Bhattacharyya and Gasparini[7] which yielded anomalous behavior of the effective mass at coverages of ^{3}He-^{4}He where a lateral phase separation of the ^{3}He at the ^{4}He surface was observed.

Our present work verifies, at least qualitatively, the observation of a two-step superfluid transition, and yields values of the ^{3}He effective mass and binding energy which complement those of the specific heat. The region of anomalous behavior has, in fact, not been explored at this point. Our present results for the effective mass show a nice consistency with the specific heat. They show for the first time a crossover behavior whereby the effective mass at constant ^{3}He coverage peaks near monolayer coverage of ^{4}He. This is the point at which a two-step superfluid transition is observed. Asymptotically the effective mass goes over to the value obtained for the infinite thickness limit—the bulk ^{4}He surface; and, in the opposite extreme, in the absence of all ^{4}He, to the bare ^{3}He mass. In the submonolayer region we believe that the theory of Pandharipandi and Itoh[26] for the effective mass of ^{3}He in 3D mixtures could be extended by 2D to check on these experimental results.

II. EXPERIMENTAL DETAILS

The concept of using a torsional oscillator to study properties of superfluid helium dates back to the work of Andronikashvili.[27] In this technique one makes use of the fact that a fluid will follow the tangential motion of an oscillating surface in contact with it over distances of the order of the viscous penetration depth. For superfluid helium in particular, which one may think of as consisting of a viscous component, the normal mass, and a superfluid component of zero viscosity, the moving surface is "loaded" only by the normal mass. Thus, from a measurement of the oscillator period one can determine the normal fluid component and hence the fraction which is superfluid.

The viscous penetration depth, δ, is given by[28]

$$\delta=(2\eta/\omega\rho_n)^{1/2}, \quad (1)$$

where η is the viscosity, ω the angular frequency of oscillation and ρ_n is the normal fluid density. At a frequency of 1 kHz, and near the superfluid transition, $\delta\cong 20\,000$ Å. Thus, for all practical purposes, the normal component of superfluid films, which even at saturation do not exceed ~ 300 Å in thickness, is completely locked to the oscillating substrate. An oscillator designed for such a measurement is shown in Fig. 1. It is very similar to oscillators which have been used previously.[25,29] It consists of a beryllium-copper (Be-Cu) torsional element to which is attached a cell of large surface area. This cell is made by winding a Mylar strip (2.5 μm thick by 2.4 cm wide) over a shell machined from a magnesium alloy.[30] The cell is sealed and bonded to the torsional element with epoxy.

The winding of the Mylar on the magnesium shell is done at minimum tension of the strip and with periodic spraying of a very dilute suspension of 0.3 μm alumina powder in methanol. This procedure visibly relaxes the static cling of the Mylar, and has been found empirically to yield cells where the area measured by nitrogen adsorption isotherms agree well with the calculated geometrical area. Cells which are wound with too much tension yield adsorption areas which are less than the geometrical

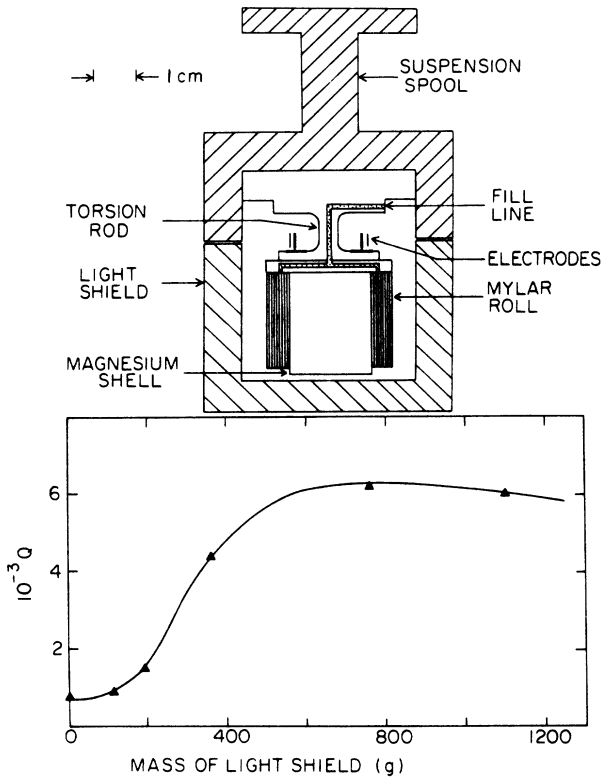

FIG. 1. Schematic of the torsional oscillator arrangement. The suspension spool is bolted to a fixed which holds the magnetic thermometer. The whole unit is connected to the mixing chamber of a dilution refrigerator. Bottom: variation of the oscillator Q in air is function of the mass loading on the light shield.

area. It is thought that the alumina acts as a spacer for the Mylar, but this is not clear. The amount used contributes negligibly to the total surface area. The Mylar roll is epoxied at its edges and at its outer surface to the magnesium shell. This is done to prevent movement and avoid random changes in moment of inertia.

The arrangement of the oscillator and its suspension are shown in the upper part of Fig. 1. The torsional element is machined out of BeCu and then annealed for three hours at 316 °C in an argon atmosphere. Two electrodes are epoxied to it and match stationary electrodes which are attached to the suspension spool. These electrodes form capacitors for driving the oscillator and picking up its angular displacement. The suspension spool is bolted to a fixture which contains the Cerium Magnesium Nitrate thermometer and a calibrated Ge thermometer. This whole unit is then suspended from the mixing chamber of a dilution refrigerator. The suspension spool provides vibration isolation for the cell by acting as a low pass filter. The resonance frequency of the suspension is $\lesssim$200Hz, well away from the cell resonance $\sim$1.4 kHz.

The Q of the oscillator, the ratio of the stored mechanical energy to energy lost per cycle, is an important figure of merit. Oscillators of high Q tend to be more stable in frequency and are sensitive to smaller loss mechanisms in the system of interest, the helium film. Intrinsic losses for an oscillator, arranged as in Fig. 1, come from a number of sources: the Mylar cell itself, the electrode structure, the capillary attached to the filling line, various bolted joints, electrical leads and residual coupling to external vibrations. After insuring that all mechanical joints, wires, etc., are secured, we empirically tuned the oscillator suspension as much as possible away from external influences. This was done by varying the mass of the light shield. A plot of the resulting Q of the oscillator as function of light-shield mass is shown in Fig. 1. As one can see, this "tuning" procedure has quite a dramatic effect on the Q. For our experiment we used a mass of 1 kg. The oscillator has a Q of 6×10^3 in air at room temperature. This improved to 2.5×10^5 in vacuum at 4.2 K. This Q is the same as that obtained with a similar cell built by one of the authors (FMG) and Agnolet.[29] We believe that this value of Q is representative of this type of cell design rather than being limited by other factors such as the Be-Cu rod or other influences. Be-Cu torsional elements can yield Q's which are substantially higher. Values as high as 1.6×10^6 have been obtained in our laboratory when the cell is replaced by a Be-Cu load of equivalent moment of inertia or a rigid silicon cell.

The circuit to drive and detect the resonance of the oscillator is shown in Fig. 2. This is a phase-locked loop in which the oscillator is the frequency determining element. A displacement at the pickup electrode C_1 yields a signal V_s which, in the limit of $R\omega(C_1+C_g)\gg1$, is given by

$$V_s = V_1 \frac{C_1}{C_1+C_g}\frac{d_1}{d_0}\ , \tag{2}$$

where V_1 is the dc bias, C_g is the capacitance to ground (in practice $C_g \gg C_1$), and d_1 is the displacement of the

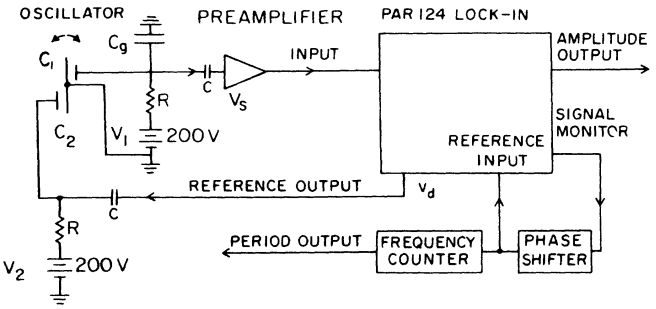

FIG. 2. The electronic arrangement for a constant voltage drive. The mechanical oscillator is the frequency determining element in a phase-locked loop.

electrode from its equilibrium value of d_0. The signal is processed through a PAR124 lock-in detector operating in internal mode. The dc output of the lock-in is proportional to the oscillating amplitude, and hence the Q. The signal monitor provides the input for the reference channel after a suitable phase shift to achieve resonance condition. The phase shifter also drives a frequency counter to monitor the period. The output from the reference is used to drive the oscillator. The dc bias at C_2 insures that the driving force has a frequency component at resonance. We also often used in this circuit a *phase meter* to monitor the phase change between the signal monitor output and the reference output. This, as we shall see, is also related to the oscillator Q.

In Fig. 3 we show a strip chart recording of the period of the oscillator over an eight hour time interval. The temperature is regulated at 0.363 K and the experimental cell is loaded with a helium sample as indicated. Over the time interval shown here we detect a total period drift of about one part in 10^8. This is roughly twice our best period resolution with a few minutes averaging time. If this drift in period were due to a movement of ^{3}He in or out of the cell, it would amount to a change of 1.4×10^{-3} layers, i.e., 0.14% of the amount present for the data of Fig. 3. In practice, in a course of a measurement the oscillator might suffer sudden shifts in period much larger

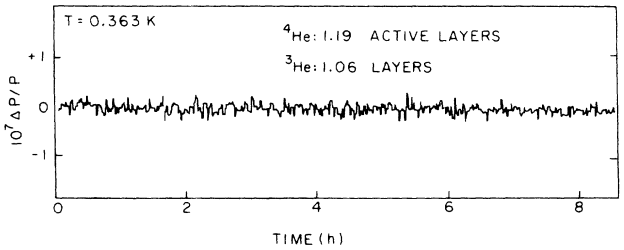

FIG. 3. An example of the oscillator long term period stability. Each period update is averaged for about 100 s.

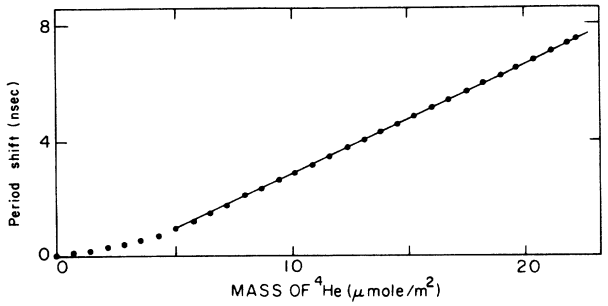

FIG. 4. Loading of the oscillator to determine the mass sensitivity. The nonlinear initial behavior represents inhomogeneous initial films. All coverages shown in this figure are for nonsuperfluid films. The period shift is measured relative to the empty cell.

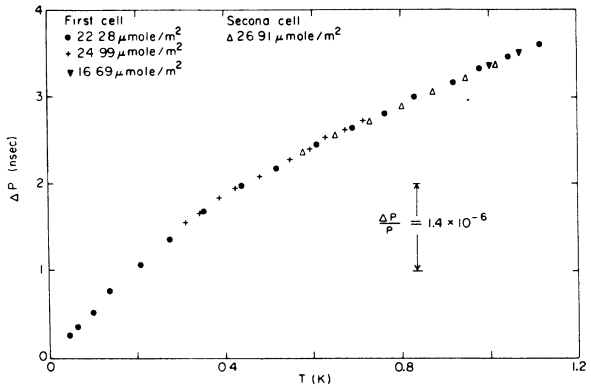

FIG. 5. Temperature dependence of the oscillator period when loaded with a nonsuperfluid film. The various data are shifted to agree at one point.

than the above, especially if the cryostat is disturbed such as in the transferring of liquid helium. These shifts are typically not important since for most of our measurements only relative changes matter.

The mass sensitivity of the oscillator is determined by measuring the period shift upon addition of ^{4}He. The results from such a measurement are shown in Fig. 4. Here we have plotted the oscillator period shift as function of the amount of ^{4}He added. After an initial nonlinear behavior, which we believe is due to an initial nonuniform coverage (we did not anneal these films by raising the temperature of the cell), the period obeys an expected linear relation. From this we determine $dP/dN_4 = 47.7 \pm 0.3$ μsec/mol ^{4}He. This agrees rather well with our estimate of 47 ± 1 μsec/mole based on the geometry of the oscillator. The data shown in Fig. 4 are normalized by the surface area of the oscillator. This, which is due almost entirely to the Mylar, is determined via a Brunauer, Emmett, and Taylor analysis of nitrogen adsorption isotherms.[31] The area is 7.85 ± 0.08 m^2. This was determined before the cell was cooled down and again after it was warmed up to room temperature. These data yielded the same area. In our work we have used two experimental cells. The second cell had an area of 6.46 ± 0.06 m^2.

For thermometry in our experiments we have used the magnetic thermometer built by Bhattacharyya and a commercial calibrated germanium thermometer. Details of the thermometry can be found in Refs. 22 and 32.

III. DATA

When ^{4}He is first physisorbed on a surface at low temperatures, it is known that typically one and two atomic layers of the helium do not become superfluid. It is only for coverages exceeding this inert layer that a superfluid transition is observed.[13] For instance, the data shown in Fig. 4 are all for coverages where, even if the cell is cooled to the lowest temperature accessible to us, 0.04 K, no transition is observed. For situations where there is no superfluid in the cell, the temperature dependence of the oscillator is very similar. Some of these data are shown in Fig. 5. Here we have plotted relative changes in the period for data of various coverages of our two experimental cells. These data are made to agree at a single point at the lowest temperature. Taken together these data determine a background dependence of the oscillator which is subtracted from the dependence observed in the presence of the superfluid. A similar situation pertains to the amplitude as well, which, in fact, changes almost negligibly in our region of interest.

When the helium film does become superfluid, an example of the oscillator behavior with the background removed is shown in Fig. 6. In the lower panel of this

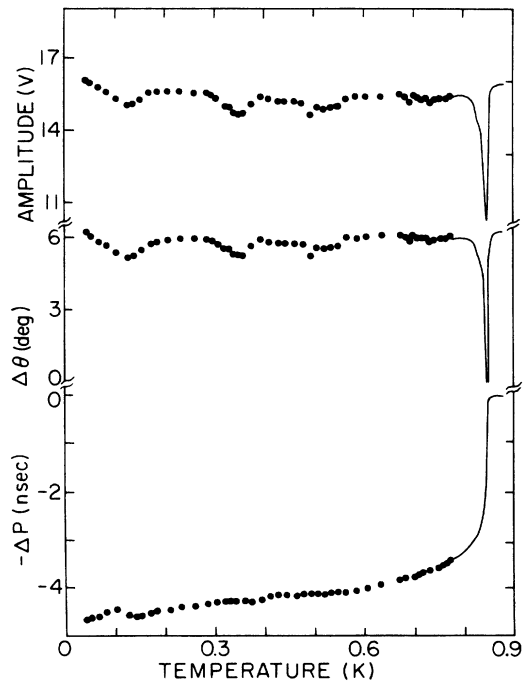

FIG. 6. Oscillator amplitude, phase, and period variations in the case of a helium film becoming superfluid. The peak in dissipation is at 845.1 mK. The dense data points near the transition have been replaced with continuous lines.

figure, the changes in the period reflect the fact that at 845.1 mK the film has become superfluid and has begun to decouple from the oscillator. The total change in period, from above the transition to $T=0$,

$$\Delta P(0)=P(T>T_c)-P(0) ,$$

should be due to the total mass of helium above the inert layer becoming superfluid. In fact, a portion of the superfluid remains locked to the substrate due to roughness or geometric constraints. This portion, denoted by χ, can be determined from $\Delta P(0)$ and the expected $\Delta P(0)$ based on the amount of helium condensed and the mass sensitivity of the oscillator as determined from Fig. 4. We find for our oscillator that $\chi=0.028\pm0.004$ independent of ^{4}He coverage. Thus, the superfluid mass, m_s, at any temperature can be written as

$$m_s(T)=\Delta P(T)/[(1-\chi)dP/dm] , \quad (3)$$

where $dP/dm=\frac{1}{4}dP/dN_4$. The upper two panels in Fig. 6 show the changes in signal amplitude A and phase difference θ between the oscillator drive and pickup signals. These quantities are related to the Q as follows:[33]

$$A=A_0Q(1-\tfrac{1}{4}Q^2)^{-1/2}\cong A_0Q , \quad (4)$$

$$\tan\theta=2Q(1-\tfrac{1}{2}Q^{-2})^{1/2}\cong 2Q , \quad (5)$$

where the last expressions are appropriate for high enough Q, 2.5×10^5 in our case. A_0 is related to the amplitude of the drive signal and the stiffness of the torsional element. θ is close to 90°. For small changes over a temperature region where the elastic property of the torsional element is constant, one has

$$\Delta A=A_0\Delta Q . \quad (6)$$

Thus, at fixed drive amplitude, changes in the amplitude of response are directly proportional to changes in Q. In the case of the phase we measure an angle $\phi=\theta+\gamma$, where γ is a phase shift introduced in the electronic loop. As long as γ in constant we still have

$$\Delta\theta=\Delta\phi=2\Delta Q\cos^2\theta , \quad (7)$$

hence small changes in θ are also proportional to changes in Q. Note as well that via $\Delta\theta$, one can, in principle, determine ΔQ even if the oscillator drive is not constant.

The sharp change in Q visible in Fig. 6 takes place at the superfluid transition and is indicative of the extra dissipation in the helium film due to motion of vortices. Detailed quantitative analyses of the dissipation and superfluid mass near the transition have provided tests of dynamic theories of the superfluid transition in two dimensions.[25,29]

The additional bumps and wiggles seen in the Q at temperatures below the transition are in some cases random disturbances, in others they are quite repeatable and correlate, as well, with structures in the period. In such cases, this additional dissipation is likely to come from excitations in the film such as third sound resonances.

Using data such as those in Fig. 6, one can determine the superfluid transition temperature as function of ^{4}He coverage. To first order, one may identify the transition as the temperature at which the dissipation peaks. In fact, it is known that the transition temperature one would measure at zero frequency is below the dissipation peak.[25] This need not concern us here since we will not do a quantitative analysis of the data near the transition. We show in Fig. 7 a plot of the transition temperature as a function of ^{4}He coverage. A smooth curve is drawn through these data and it extrapolates to 25.8 μmol/m^2. This number, which we identify as the inert layer, can be compared to other results for a Mylar substrate, 24.9 and 27.8 μmol/m^2 (Refs. 25 and 29). Our results corresponds to 1.99 atomic layers of bulk helium at zero pressure (12.97 μmol/m^2), or roughly 1.5 atomic layers if one allows for density variations due to the compression of the helium at the adsorbate surface. We have also plotted in Fig. 7 the magnitude of the period change from above the transition to $T=0$, $\Delta P(0)$. We see that this is linear in coverage of ^{4}He and intercepts the axis at the same point as the curve defined by T_c. Thus, $\Delta P(0)$ determines the same inert layer.

We can compare our results for T_c as function of coverage *above* the inert layer with other work. This is shown in Fig. 8. The original data by Bishop and Reppy[25] show a very nearly linear dependence of T_c on coverage; our own data (run 1,4,5), through which we have drawn a smooth curve, has a negative curvature; and those of Agnolet and Reppy show a somewhat more complex behavior.[29] It seems clear that although all of these data follow a general trend, they do not overlap within the expected errors of determining T_c, the coverage (which involves determining the adsorption area), or the value of the inert layer. These differences cannot be ex-

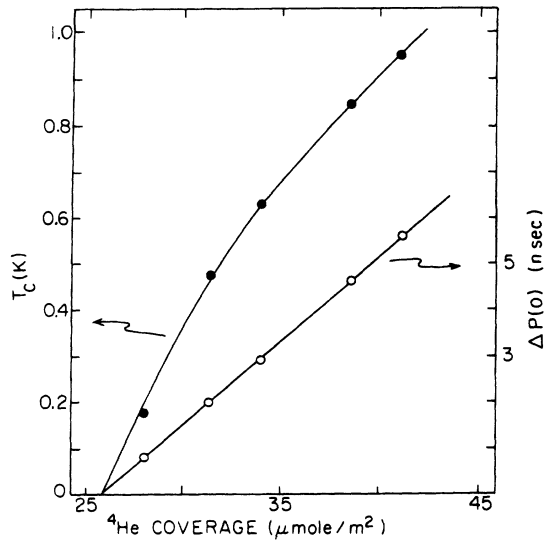

FIG. 7. The transition temperature T_c, and total period shift from $T>T_c$ to $T=0$, $\Delta P(0)$, for several coverages of ^{4}He. The lines through the data intercept the ordinate at 25.8 μmol/m^2. Only for coverages above this value does one have a superfluid film.

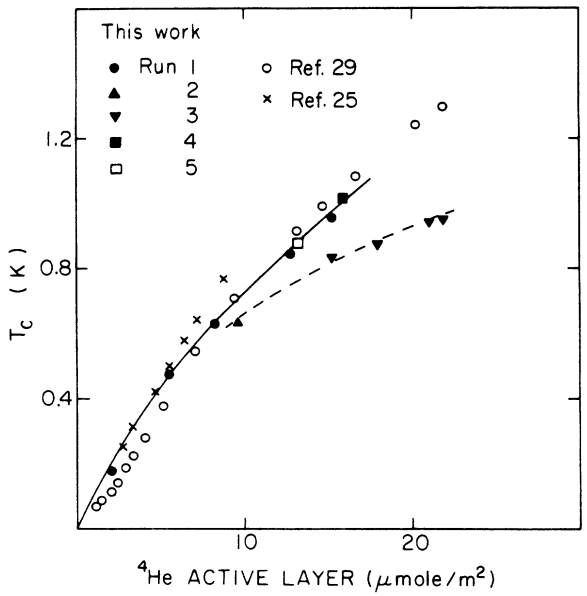

FIG. 8. The transition temperature as function of coverage above the inert layer, as determined from Fig. 7.

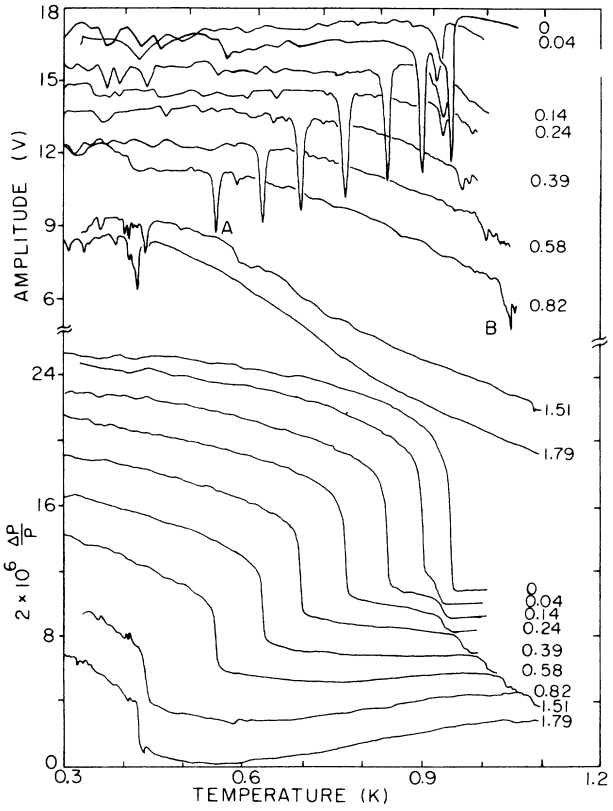

FIG. 9. Period and amplitude variations due to the mass loading with a 1.19 layer of ^{4}He and various coverages of ^{3}He ranging from 0.04 to 1.79 atomic layers. The dissipation peak at transition B has been plotted at twice the sensitivity as that of transition A.

plained away by vapor corrections—these are negligible for the data below ~ 1 K. There appear to be residual systematic differences which are unique to each experimental cell. In our case, we note that runs 4 and 5 (the squares) were done with a different experimental cell from run 1. These data seem reasonably consistent with those of run 1. The marked deviation from the general trend displayed by the data from our run 3 and to some extent run 2, which we have joined with a dashed line, we believe are due to inhomogeneous films. We will return to this point later.

In Fig. 9 we show a subset of the results obtained in our first experimental run to determine the superfluid transition in mixture films. A more complete set of just the period data for this run has already been published.[34] What is plotted in this figure is the amplitude of the oscillator and the fractional period change. The quantity $2\Delta P/P$ plotted this way is proportional to the superfluid mass.[25] These data start with a pure ^{4}He film of 15.37 μmol/m^2 of 1.19 active layers. T_c for this film is at 949.9 mK. Upon addition of small amounts of ^{3}He, which is indicated on Fig. 9 in units of atomic layers, it is seen that the transition from the normal to the superfluid state takes place in two steps. Coincidental with each of the steps in the period the amplitude signal shows an increase in dissipation. This dissipation is much more marked for the A transition than the B. The smaller dissipation at B is of course consistent with the smaller period change at B indicating that a smaller portion of the film is involved in this transition. For emphasis we have actually plotted in Fig. 9 the dissipation at B at twice the resolution of A. We have designated these transitions after the convention used by Bishop and Reppy who were first to report a two-step transition in a mixture film.[25] As we continue to add ^{3}He (1 layer $\equiv 6.4\times10^{14}$ cm^{-2}) transition B moves to higher temperatures and eventually *exceeds* T_c of the pure ^{4}He film. The main transition, A, shifts to lower temperatures. Eventually, at coverages close to 1.5 layers of ^{3}He the B transition is no longer identifiable. A plot of the temperatures at which the dissipation peaks as function of ^{3}He molar concentration, x, is shown in Fig. 10. Here we have also plotted the results for transition A of two other runs done with the second cell. The peak dissipation temperature, $T_c(x)$, is normalized by $T_c(x=0)$. We calculate the concentration of ^{3}He by using only the number of ^{4}He in the active layer of the film, not in the total ^{4}He coverage, i.e., we do not include the solid layer. This concentration represents an average value and not the value which is appropriate for phase A or B. We do not have enough experimental information to calculate these separately.

The trend shown by transition A is a nearly linear initial shift, initial slope -1.25 ± 0.14, and a much shallower slope at higher concentrations. This latter behavior which is even more striking if one plots the data as a function of atomic layers of ^{3}He (see Ref. 23) is due to the gradual buildup of the ^{3}He overlayer on the superfluid film. As this overlayer builds up it has less and less influence on the transition temperature of the underlying ^{4}He (Refs. 4, 24, and 34). The initial slope of transition A

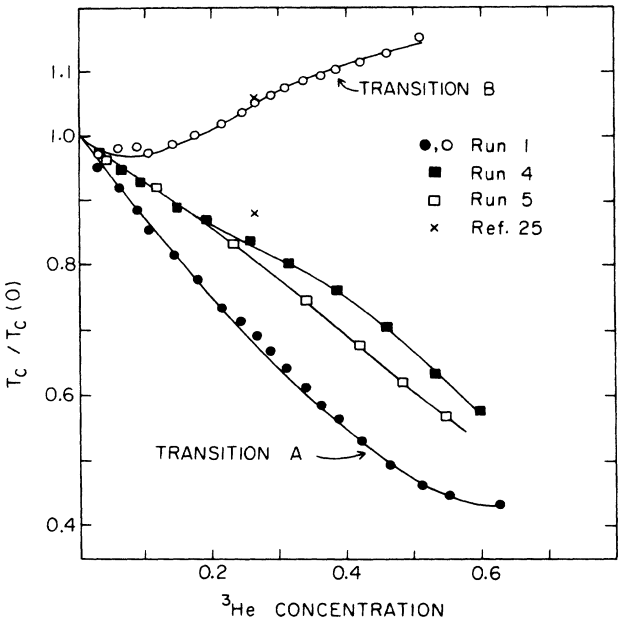

FIG. 10. The temperature of maximum dissipation T_c, normalized by the value for the pure film, as a function of ^{3}He concentration.

can be compared to a value of -0.73 ± 0.03 obtained from the data of runs 4 and 5, which all have initial ^{4}He coverage of near one atomic layer, and values of -0.88 and -0.95 for data with initial coverage of less than one monolayer, $T_c(x=0)$ of 0.221 and 0.537 (Ref. 35). Theoretical values for two-dimensional mixtures of ^{3}He in ^{4}He tend to be somewhat larger.[15,16,36] We will return to this later.

The locus of transition B seems rather more complex with $T_c(x)$ first falling below $T_c(0)$ then rising above it before becoming unidentifiable near 50% concentration. The point from the work of Bishop and Reppy[25] agrees with these data, but this is more likely fortuitous given that their fractional shift of transition A is not in agreement with ours.

We have interpreted transitions A and B as resulting from regions where the superfluid film has two different values of thickness (or density) and concentration. The transition into these phases must take place at temperatures above the superfluid transition A, or these phases must be the equilibrium configuration for the particular ^{3}He-^{4}He coverages we are studying. This latter possibility is analogous to the existence of the ^{3}He surface state for the free surface of bulk ^{4}He, or of thicker ^{4}He films. This then would not represent a phase transition. We note that with our oscillator we are not sensitive to mass redistribution within the helium film as long as the ^{4}He is normal. Thus, if a separation into phases A and B took place above the superfluid transition A, we would not see it.

It remains a question now whether phases A and B are an intrinsic feature of the mixture films or somehow a result due to some peculiar features of our cell. If the latter were the case, then the pure ^{4}He films should show similar structures to what is observed with the mixture. The evidence is to the contrary. The mass loading studies, see Fig. 4, show good linearity in the formation of the inert layer. Further, when the superfluid film does form, a single transition is observed, and at T_c we obtain the right value[37] for the universal jump as expected from the Kosterlitz-Thouless theory.[38] Thus, we have concluded that it is the addition of ^{3}He which is responsible for the formation of regions of different ^{4}He coverage and concentration. This view is supported, as well, by our analysis of the effective mass which we shall discuss later.

On the basis of the preceding interpretation, we have analyzed our mixture data to test whether, as in the case of the pure films, they obey the theoretical prediction of a universal jump in the superfluid density per unit area:[38]

$$\frac{\Delta M_s}{ST_c}=3.49\times10^{-9}\ \text{g/K cm}^2\ . \tag{8}$$

In our case, with two transitions, we have the constraint that

$$S=S_A+S_B=7.85\ \text{m}^2$$

and

$$\Delta M_A/S_AT_A=\Delta M_B/S_BT_B\ .$$

These two equations allow us to calculate S_A,S_B, and, hence, the universal ratio. The result of this calculation have been reported in Ref. 34. The data are well described by this analysis and give a value of $3.55\pm0.1\times10^{-9}$ g/K cm^2, in good agreement with Eq. (8). We note that the area occupied by phase B ranges from 18% to about 8% of the total as the ^{3}He coverage varies from its lowest to highest value.[37] Also, we remark that phase B must correspond to a larger ^{4}He thickness (or density) than the average of 1.19 layer. This, in turn, implies that the data for transition A should be plotted in Fig. 10 at somewhat higher concentrations. This would tend to give these data a somewhat shallower slope than indicated in this figure and more in agreement with films which do not display a two-step transition into the superfluid state.

The region between transitions A and B is also of interest. As the concentration, or coverage, of ^{3}He is increased, this region widens and changes in character (see Figs. 9 and 2 of Ref. 34). At first, at low coverage, there is an increase of mass loading with temperature, which in a sense is a precursor to transition B much like the increase in mass loading precedes the sudden transition at A. At higher coverages, however, this behavior changes rather dramatically. For the data of 1.51 layer, for example, $\Delta P/P$ changes by $\sim10^{-6}$ in going from 0.6 to 1.05 K in a direction indicating a *decrease* in mass loading. This is concomitant with an increase in the dissipation.

Changes of mass loading and dissipation can come from a variety of mechanisms within the cell. All of these involve movement of ^{3}He from one phase to another or from regions where the ^{3}He follows the movement of the substrate to where it does not. These could be regions within the cell which are farther than a viscous

penetration depth from the oscillating surface or into the connecting line to the cell which has a low-temperature volume of about 1 cm^3. It is likely that a number of mechanisms are involved, but analysis of our data suggests that a simple evaporation mechanisms is the dominant effect. We can make this more quantitative as follows. We assume after Bhattacharyya *et al.*[5] that the ^{3}He in the ^{4}He film can be described as a two-dimensional Fermi gas bound with an energy ε relative to the vacuum. We further assume for simplicity that a single bound state exists for the ^{3}He in this very thin ^{4}He film. Then, the number of atoms in the film of area S and in the vacuum of volume v are given by

$$N_f = g_f T \ln\{1+\exp[(\mu+\varepsilon)/T]\} , \quad (9)$$

$$N_v = g_v T^{3/2} \exp(\mu/T) , \quad (10)$$

where $g_f = 4\pi m S k/h^2$ and $g_v = 2v(2\pi m_3 k/h^2)^{3/2}$, and μ is the chemical potential. The masses m, m_3, are, respectively, the effective mass of the ^{3}He in the film and bare mass in the vacuum. From the preceding equations we should, in principle, be able to obtain values of ε and m from the observed variation in the oscillator period. This, in fact, is difficult because the period variations due to movement of the ^{3}He are superimposed to changes due to the superfluid mass. In the case of the dissipation, however, the situation is more favorable since changes of dissipation due to the superfluid transition are localized principally near T_c. We can proceed as follows.

For a plane oscillating with velocity $u = u_0 \cos(\omega t)$ in a fluid of viscosity η and density, ρ, the energy dissipated per unit time and unit area, δE, is given by[28,39]

$$\delta E = \tfrac{1}{2} u_0^2 (\tfrac{1}{2}\omega\eta\rho)^{1/2} . \quad (11)$$

Since the energy stored in this oscillator is $\frac{1}{2} I u_0^2/R^2$, where I is the moment of inertia and R an effective radius of the cell (~ 1.5 cm). Then, the quality factor due to the gas in the cell is

$$Q_{\text{gas}} = I/R^2 A (\pi P \eta \rho)^{1/2} , \quad (12)$$

where A is the portion of the area of the cell above which the gas is farther away than a viscous penetration depth. To test Eq. (12) with the experimental data, we note that the total measured dissipation in the oscillator, $1/Q$, is the sum of an intrinsic value, $1/Q_{\text{in}}$, plus that due to mechanisms associated with the helium film and gas. Since, away from the transition the film contributes little to the dissipation, we may write to a good approximation

$$\frac{1}{Q} = \frac{1}{Q_{\text{in}}} + \frac{1}{Q_{\text{gas}}} . \quad (13)$$

Now by using Eq. (2), and the fact that $Q_{\text{in}} \cong 2.5\times 10^5$, we write Eq. (12) as

$$2.5\times 10^5 \left[\frac{V_{\text{in}}}{V} - 1\right]^{-1} = I/R^2 A (\pi P \eta \rho)^{1/2} , \quad (14)$$

where the V's are the measured voltage signals. To test the data we must solve Eqs. (9) and (10) for N_v, and thus $\rho = N_v/v$. This can be done most simply if N_v is much larger than the total number of ^{3}He condensed, N_T. In this case we have

$$N_v = [\exp(N_T/g_f T) - 1] g_v T^{3/2} \exp(-\varepsilon/T) . \quad (15)$$

Placing this result in Eq. (14) we obtain

$$-\frac{\varepsilon}{2T} = \ln\left[\frac{(V_{\text{in}}/V - 1)}{[\exp(N_T/g_f T) - 1]^{1/2} T^{5/4}}\right] + \ln(g_0 g_v^{-1/2}) , \quad (16)$$

where

$$g_0 = 4.3\times 10^{12}/AK^{-3/4} .$$

This number incorporates all the constants appropriate for our oscillator [see Eq. (14)] and the viscosity of the ^{3}He gas which we have taken as $\eta = 7\times 10^{-6}$ T g/cm sec K (Ref. 40). Equation (16) is appropriate for the limit where the viscous penetration depth is much larger than the mean free path of the ^{3}He in the gas and much shorter than the separation between the Mylar surfaces at the places where the dissipation takes place. Further, the assumptions leading to Eqs. (9) and (10) would also fail for ^{3}He coverages approaching one atomic layer. For all of these reasons, Eq. (16) is useful only for intermediate ^{3}He coverages near one-half of an atomic layer. We show the results of plotting the right-hand side of Eq. (16) versus $1/T$ in Fig. 11. These data, for a range of ^{3}He coverages

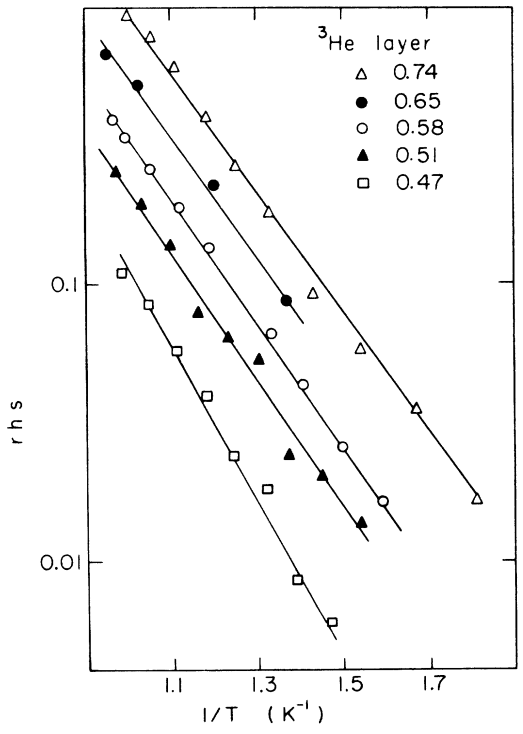

FIG. 11. The right-hand side of Eq. (16) plotted vs $1/T$. The data for each coverage of ^{3}He are shifted relative to each other for clarity. The slopes of these lines yield the ^{3}He binding energy to the ^{4}He films.

between 0.74 and 0.47 layer, fall on reasonable straight lines as expected. The area required to give the dissipation represented by all of these data is $A = 200 \pm 100$ cm^2. This is a small fraction of the total surface area of 7.85 ± 10^4 cm^2. From the slopes of the lines in Fig. 11 we obtain values of ε which are plotted in Fig. 12. Here we have also plotted values of the ground-state energy from the specific-heat data of Bhattacharyya *et al.*[5] The present data yield higher values, $\varepsilon \cong 10-12$ K as expected for a thinner ^{4}He film. The general trend of these data is for ε (ε_1 in the notation of Ref. 5) to decrease with coverage of ^{3}He. This perhaps reflects a slight compression of the film as ^{3}He is added. The exception to this are the data at low coverage for 10 Å which are discussed in Ref. 7.

It is not quite meaningful to compare the values of ε with theoretical estimates since these apply to the zero coverage limit. It is also not clear that such theories should apply to such a very thin ^{4}He film as in our present work. Nevertheless, we note that $\varepsilon \sim 10$ K is quite a reasonable result based on the theory of Refs. 18, 19(a) and 19(b). We conclude then that our description of the dissipation away from the transition in terms of ^{3}He evaporation is quite sensible.

After obtaining the data on the two-step superfluid transition described earlier, and since data with both submonolayer mixtures and multilayer mixtures show a unique single-step transition into the superfluid state, we proceeded under the assumption that the two-step transition which we observed was connected with the fact that we were dealing with an active film near one atomic layer thick. To verify this conjecture, we started in a second run with a coverage below one active layer of ^{4}He and examined the transition upon addition of ^{3}He. Some of these data are shown in Fig. 12. The pure ^{4}He film has a T_c of 626 mK. Upon addition of ^{3}He, this transition shifts to lower temperature and loses its sharpness by developing a post-transition "tail". When the ^{3}He coverages reaches 0.35 atomic layers (the total coverage is now 1.1 atomic layers of ^{3}He and ^{4}He), there seems to be a hint of a second step, but clearly not in the same conclusive way as the data of Fig. 9.

After these observations, we changed our thermodynamic path and, instead of adding ^{3}He, we increased the ^{4}He coverage. In this way we would reproduce some of the results of the first run. These additional data look very similar to the data of Fig. 13, but with the main transition moving up in temperature.[41] A somewhat sharper small transition develops where the ^{4}He coverage is 1.2 layer, as in the first run. However, this transition temperature does not match the one of the first run.

These observations suggest to us that in this second run the film coverage is not uniform. The gradual decrease in mass loading above the transition shown in Fig. 13 could come, for instance, from a distribution of film thickness. What is somewhat surprising is that the pure ^{4}He film data, apart from the fact that its T_c is somewhat lower than those obtained from the first run (see Fig. 8), show a rather well-defined transition with no tail above T_c. It is only upon addition of ^{3}He that this develops.

In a third run with the same experimental cell, we first made a series of measurements with pure ^{4}He films. Their T_c's as function of active film coverage are also shown in Fig. 8. These transition temperatures are very substantially *below* the trend established for our first run

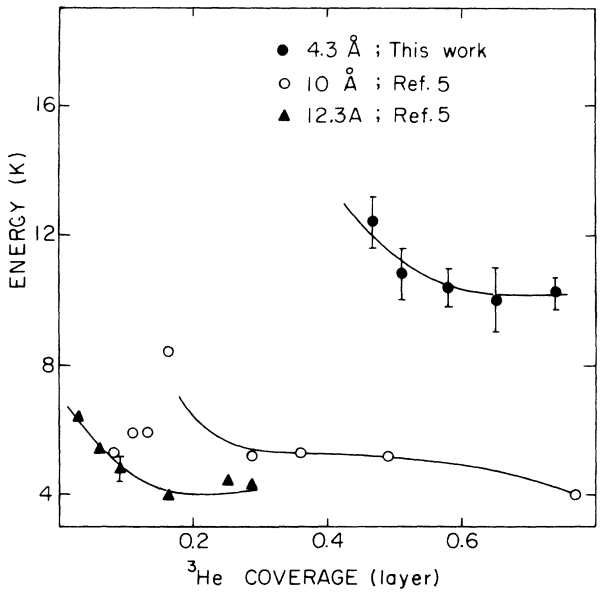

FIG. 12. The ^{3}He binding energy as a function of ^{3}He coverage as obtained from Fig. 11. Other data for different ^{4}He thickness are from the heat capacity measurements of Ref. 5.

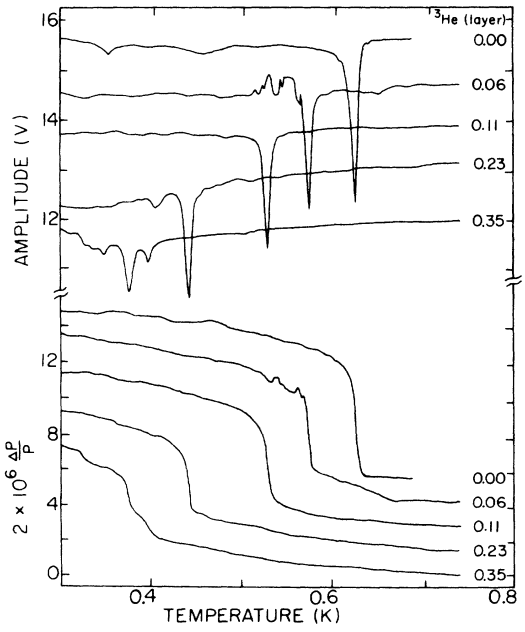

FIG. 13. Period and amplitude variations due to the mass loading of the oscillator with a film of $T_c = 626$ mK. The ^{3}He coverage is indicated next to each curve. These are data obtained in a second run with cell 1.

suggesting again that the films are not uniform and that more helium is necessary to achieve the equivalent T_c's of the first run. Upon addition of ^{3}He to the ^{4}He film with highest T_c, 943 mK, similar results to the second run were obtained.[37]

It seems clear to us that between the first and subsequent runs the conditions in the experimental cell had changed. It seems quite plausible that upon recycling between low temperature and room temperature, shifts and relative movements in the Mylar substrate would occur. One might expect that these would effect thick-film homogeneity by providing regions where the helium would capillary condense, but, what seems somewhat surprising is that they would affect the homogeneity of the near monolayer films. To pursue our studies further, we built a new experimental cell. This was made similarly to the previous cell except that the Mylar ribbon was wound somewhat more loosely.

Some of the results from a first run using this second cell are shown in Fig. 14. These data are for a ^{4}He film of 1.22 active layers, $T_c=1.010$ K. Note from Fig. 8 that the T_c for this film is in good agreement with the T_c's established during the first run with the first cell. Upon addition of ^{3}He to this film we see no evidence of transition B until we exceed 0.15 layer of ^{3}He coverage. Beyond this, we can see that transition B is again well defined. This persists for ^{3}He coverages up to about 0.7. At higher coverages this transition tends to be washed out. The locus of $T_c(x)/T_c(0)$ for transition A as function of ^{3}He concentration is shown in Fig. 10. As we remarked earlier, the fractional shift in T_c is not as rapid as in the first run. For transition B the locus of $T_c(x)/T_c(0)$ is nearly constant at about 0.9. The dissipation peaks associated with transition B are plotted in Fig. 14 at three times the amplitude resolution for transition A. These peaks at B, as well as the period steps, are thus weaker than those in Fig. 9. From an overall comparison of these data we conclude that while they give good evidence for a two-step superfluid transition for what is very closely the same ^{4}He film (1.19 and 1.22 layers), there is still lack of quantitative agreement.

In an additional run with the second cell, we measured a ^{4}He film of 1.03 active layers, $T_c=0.869$ K. In this case, we found that although small steps, at times more than one at a given coverage, were observed in the oscillator period, these did not correlate unambiguously with the dissipation signal. These data are shown in Fig. 15. We conclude that there were no clear cut indications of transition B for this coverage of ^{4}He. Interestingly, the fractional shift in the transition temperature for this run agrees with the previous run at low coverages where, as well, no transition B was observed.

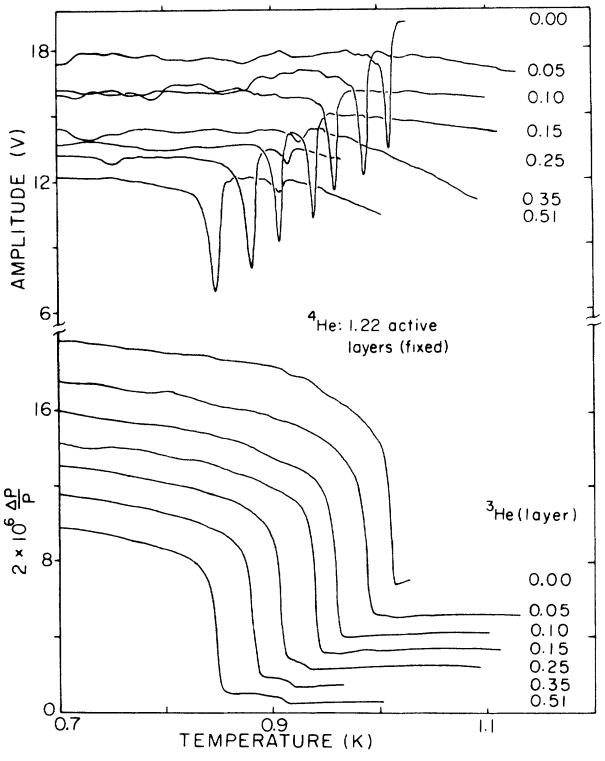

FIG. 14. Period and amplitude variations due to the mass loading of the oscillator with a film of $T_c=1.01$ K. The ^{3}He coverage is indicated next to each curve. The dissipation peak associated with the higher temperature transition is plotted at three times the resolution of the main dissipation signal. These data are from our fourth run and were obtained with cell 2.

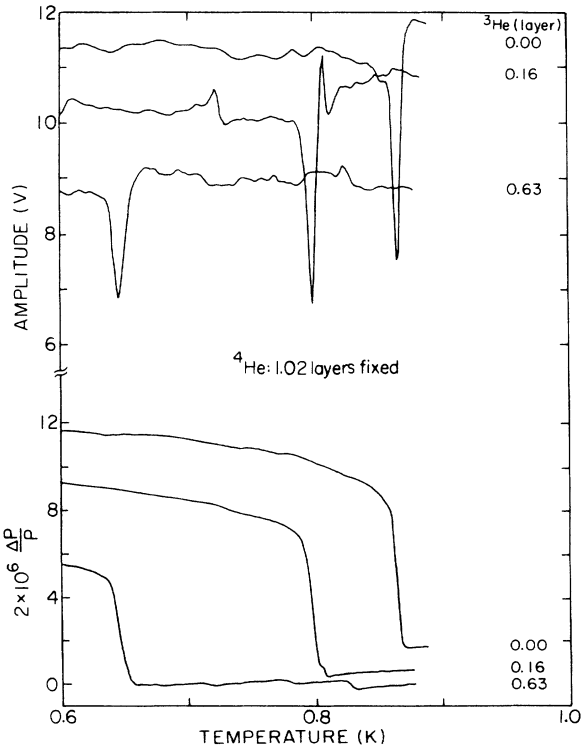

FIG. 15. Period and amplitude variations due to the mass loading of the oscillator with a film of $T_c=865$ K. The ^{3}He coverage is indicated next to each curve. These data are from our fifth run and were obtained with cell 2.

We summarize our observations of a two-step superfluid transition in mixture films as follows. In runs with two different experimental cells at coverages near 1.2 active ^{4}He layers, we see well defined signatures of these transitions. These measurements support the observation made on a single mixture film by Bishop and Reppy. At lower coverages of ^{4}He, or in situations where independent evidence (the position of T_c for the pure films as function of coverage) suggest that the ^{4}He film is not homogeneous, the second transition disappears or its identification is ambiguous.

IV. THE ^{3}He EFFECTIVE MASS

It is well known that ^{3}He as an impurity in bulk superfluid ^{4}He acts as a Fermi quasiparticle of effective mass $m \cong 2.3 m_3$. (Ref. 42). The source of the mass enhancement, at least in the dilute limit, is well understood as being due to the hydrodynamic backflow of the ^{4}He as the ^{3}He moves through it. A similar situation pertains to ^{3}He in films of ^{4}He. Results for the effective mass of ^{3}He in the case of ^{4}He films ≥ 10 Å were first obtained in our laboratory from measurements of the specific heat in the work of DiPirro and Bhattacharyya.[22,23]

As we discussed in the Introduction, the realization of what one might call two-dimensional ^{3}He in ^{4}He evolves through several stages starting with submonolayer ^{3}He-^{4}He mixtures and ending up with ^{3}He at the surface of bulk ^{4}He. The ^{3}He effective mass should differ in these various cases. We indicate this schematically in Fig. 16. Here an atom of ^{3}He is shown moving through superfluid ^{4}He in three realizations: as part of a submonolayer film; at the surface of bulk ^{4}He; and, at the surface of a film of ^{4}He several atomic layers thick. In the fully 2D realization and apart from substrate affects, a strictly 2D backflow would result as the ^{4}He moves around the ^{3}He on the surface of the substrate. In the case of ^{3}He at the surface of bulk ^{4}He, the half-space problem, the hydrodynamic backflow is not just in the surface plane but in the half space below the surface. In the third instance, the crossover case, ^{3}He is at the surface of a film. The backflow, which one may visualize as "striking" the substrate surface, is in a sense intermediate between case *a* and *b*. In fact, case *c* is even more complex because of the existence of excited states which in a sense represent motion of the ^{3}He within the body of the film.[5] In any case, on the basis of these physical arguments one would expect effective masses in case *a*, *b*, and *c* to differ. There are no theoretical calculations of m for any of these cases. In 3D the theory of Pandharipande and Itoh[26] predicts a density dependence for m which we may write as

$$m = m_3[1-\alpha\rho(P)/\rho(0)]^{-1} , \tag{17}$$

where the constant α is calculated in Ref. 26 using the appropriate He-He interaction potential. This density dependence of m has been checked experimentally and excellent agreement is found over the range of $P=0$–20 bars (Ref. 43).

With the torsional oscillator one can determine the effective mass of the ^{3}He in the following way. When ^{3}He is added to the ^{4}He film at $T > T_c$, it is locked to the substrate just like the ^{4}He. Thus, it provides a mass loading of m_3 per atom. When the ^{4}He becomes superfluid, however, the ^{3}He is still locked to the oscillating substrate, but now the ^{4}He flows around the ^{3}He and enhances the mass to m. Thus, for the mixture, the total change in period from $T > T_c$ to $T=0$, $\Delta P(0)_{\rm mix}$, is *decreased* from the value of the pure film, $\Delta P(0)$, due to the mass enhancement of the ^{3}He in the superfluid region. We may write, then,

$$\Delta P(0)-\Delta P(0)_{\rm mix} = N_3(m-m_3)(1-\chi)\frac{dP}{dm} , \tag{18}$$

where we have assumed that the same χ applies for the pure ^{4}He film as well as the mixtures. This, in practice, amounts to a $\sim 2\%$ effect. To use this equation we have to extrapolate the measured period to $T=0$. This can be done with an accuracy of about 2% of $\Delta P(0)$. N_3 is known from room-temperature measurements and dP/dm and χ are determined as discussed before.

It was shown in the work with the heat capacity that the ^{3}He effective mass is a function of both D, the ^{4}He thickness and the ^{3}He coverage. These data, however, do not extend in the full range of D to test the ideas suggested in Fig. 16. These ideas in fact should apply strictly to the limit of low ^{3}He coverage for which there are few data available. Extrapolation to zero coverage cannot be made in all cases since for certain values of D the ^{3}He undergoes a phase transition which reflects itself in an anomalous behavior of m (Refs 5 and 44). For these reasons, we have chosen to examine results for m at a ^{3}He coverage near 0.3 atomic layer for which there are a reasonable range of data available both from the specific heat and the present work. We plot these data as a function of $1/D$ in Fig. 17. In this way, case *b* of Fig. 16 can be plotted at $1/D=0$ (Ref. 45). We also include submonolayer results, case *a* of Fig. 16. In this limit D does not represent a thickness but rather a measure of monolayer completion. The values of m in Fig. 17 do indeed show different ranges of behavior, this is emphasized by the solid lines. The line at the left of the maximum is drawn to guide the eye, the line at the right is a fit to the data. (See the following.) To the left are results for multilayer films and to the right submonolayer films. The peak in m, which divides the monolayer and multilayer region, occurs near 5 Å, and it is tempting to identify this

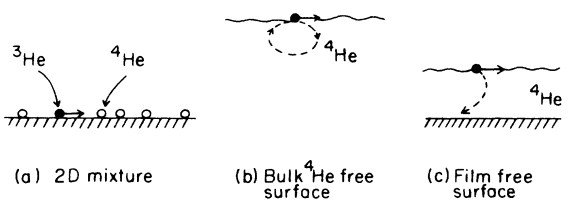

FIG. 16. Schematic representation of three realizations of mixture films: *a*, ^{3}He atom in a 2D mixture; *b*, on the free surface of bulk ^{4}He; and *c*, on the free surface of a film. The dashed lines suggest the ^{4}He backflow as the ^{3}He moves.

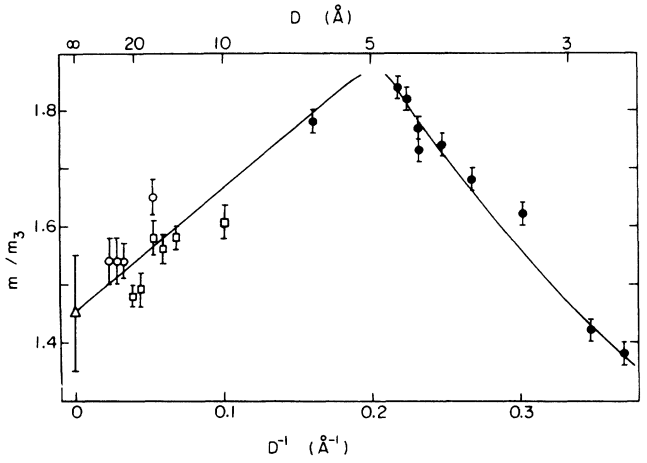

FIG. 17. The variation of the ^{3}He effective mass as function of $1/D$. The ^{3}He coverage for these data are near 0.3 atomic layers. These data represent results from surface tension (triangle, Ref. 45), specific heat open (circles and squares, Ref. 5), and the present work of oscillator mass loading (solid circles).

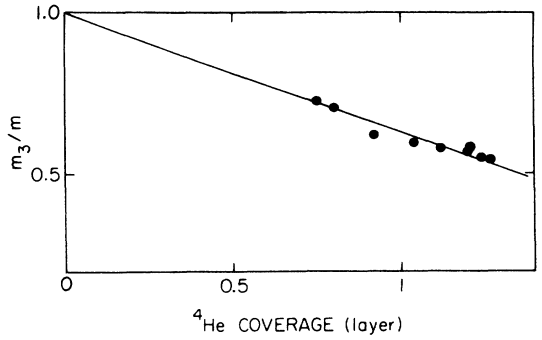

FIG. 18. Test of the dependence of the effective mass on ^{4}He density according to the functional form suggested by the 3D theory, Eq. (17).

as the formation of the first superfluid layer. This is at a somewhat higher effective thickness than 3.58 Å which would be the one layer thickness using bulk helium density. A higher value is expected due to the compression of the layer from the substrate's van der Waals attraction. Note that various sources of these data: surface tension and second sound for $1/D=0$; heat capacity for multilayers; and, the present work, torsional oscillator "microbalance" for near and submonolayer. These latter data, which are a realization of case *a* of Fig. 17, show the trend one would expect on physical grounds: The effective mass increases as the 2D ^{4}He density is increased. Finally, upon or near completion of a dense ^{4}He layer, the ^{3}He "pops out" and "floats" at the free surface. In the crossover region, case *c*, m decreases until it reaches the bulk surface value. In the submonolayer region, one might expect that an equation analogous to (17) should apply, but with the constant α replaced by a different value and $\rho(P)/\rho(0)$ replaced by σ_4, the ^{4}He layer coverage. To test this we have plotted m_3/m versus σ_4 in Fig. 18. We see that the data do fall quite reasonably on a straight line going through one at zero coverage. This point represents the case where only the ^{3}He is on the substrate, thus loading the oscillator with its bare mass. The slope of the line gives $\alpha=0.37$ somewhat lower than the 3D case as one might expect from the smaller backflow of case *a*, Fig. 16. The straight line in Fig. 17 is the same line plotted through the submonolayer data of Fig. 17.

It would be very interesting in future work to map out completely the behavior of m shown in Figs. 17 and 18. It would also be very interesting to see theoretical work to extend the calculation of Ref. 26 to two dimensions and extend this to the more difficult cases shown schematically in Fig. 16.

V. COMMENTS

There have been a number of theoretical calculations of the phase diagram for two-dimensional mixtures of ^{3}He and ^{4}He (Refs. 15, 16, and 36). The common features of these theories is a superfluid transition temperature with a fractional shift to lower values with concentration of -1 to -4. The exact number depends on the values of the coupling constants which describe the superfluid and the nonsuperfluid interactions of the helium. Experimental data of submonolayer mixtures films, as discussed in conjunction with Fig. 10, agree with these values to the extent that they are of order unity. No clear quantitative comparison can be made. Another common feature of these theories is the fact that at low temperatures the 2D mixture should phase separate. This is also true in the theory of Guyer and Miller, who consider the ground state configuration of a mixture of Fermions and Bosons.[46] These theoretical predictions have not been verified experimentally. Heat capacity measurements which are most sensitive to this have not seen phase separation.[14] Even in our own data, where the existence of a two-step transition into the superfluid state suggests that the mixture is phase separated, we have no direct measurement of where this occurs. Further, and perhaps more importantly, it is not clear that what we see is related to 2D behavior as considered theoretically, but rather to the formation of a second helium layer. This is an additional degree of freedom which the experimental system has but is not in the strictly 2D theories. The work of Mon and Saam is an exception.[36] These authors deal with a two-layer mixture film and do indeed find in certain cases two superfluid transitions. These however, are associated with each of the two layers. Again, this is not our case. Specifically, we do not have two complete layers in our measurements. Further, if transitions *A* or *B* were to be associated with a "top" or bottom layers they would have to differ strongly in T_c since the top layer would also have to be richer in ^{3}He. The magnitude of the superfluid signal of *A* and *B* would thus have to be reversed.

What seems to be closer to the mark is a suggestion made by Guyer that the helium film might find it energetically favorable to deform into regions of different ^{4}He thickness and ^{3}He coverage.[47] This mechanism was suggested to explain measurements of heat capacity done with somewhat thicker films near 3 to 4 atomic layers of ^{4}He. Although estimates by Sherril and Edwards show that to first order this mechanism is too weak to induce this kind of phase separation, it does not rule it out.[19] In any circumstance, the details of these theories do not seem to be strictly applicable to our experimental realization of a near monolayer film.

If one adds ^{3}He to a relatively dense first layer of ^{4}He, the gain in potential energy can easily be offset by the high price in the kinetic energy of confining the ^{3}He by its ^{4}He neighbors. The system relaxes from this by allowing the ^{3}He to move to an overlayer position. This mechanism is, of course, just the evolution of the surface ^{3}He layer as discussed in the Introduction. It may be possible as well, however, to have a two-phase coexistence with the ^{3}He either in an overlayer situation or "mixed" in the first ^{4}He layer. This can lead to (but does not require) two superfluid transitions in regions of different ^{4}He density. We notice that the ^{3}He effective mass tracks very nicely the formation of the first superfluid layer. m increases as the layer density increases. m decreases when ^{3}He is forced to its overlayer position. It is not surprising that if one accepts a correlation between the maximum in m and the two-step superfluid transition that the latter might be a rather delicate manifestation relying on a rather exact realization of a particular ^{4}He first-layer density. This could explain the lack of quantitative agreement between our runs 1 and 4, and the fact that in run 5 (^{4}He coverage 20% less than run 1 and 4) while there are hints of a second transition, no clear cut identification in both dissipation and period can be made.

Regarding the effective mass in the multilayer region, we note a recent calculation by Epstein and Krotscheck on the density profile of ^{4}He films on various substrates.[48,19(b)] These authors obtain profiles with marked density oscillations. The effect of these oscillations or layering of the ^{4}He film have been seen in a number of experiments.[49,50] In our own case, the ^{3}He in the ^{4}He film is in a sense a probe of the ^{4}He density via the hydrodynamic backflow. It would seem likely that more precise measurements of m would have a more complicated, i.e., oscillatory, behavior for $D > 5$ Å in contrast to the one suggested by the straight line in Fig. 17. The verification of this must await more precise results.

VI. SUMMARY

We have presented measurements of the mass loading on a torsional oscillator of ^{3}He-^{4}He mixture films. Unlike thick films and submonolayer films, we find that the superfluid transition takes place in two steps. Our data also yield values for the binding energy of the ^{3}He to the ^{4}He film and the effective mass of the ^{3}He. The data on the effective mass suggest that the two-step superfluid transition might be connected with the completion of the first superfluid layer and the formation of the ^{3}He surface state. In the submonolayer region we find that the effective mass follows a density dependence which we propose in analogy with the three-dimensional theory.

ACKNOWLEDGMENTS

We would like to acknowledge the help of D. Finotello and Y. Y. Yu in the early stages of this experiment and in the design of some of the apparatus. Francis M. Gasparini, Jr. and Steven Petrinec helped with part of the data analysis. We are grateful to D. McQueeney and J. Reppy for sharing their data on submonolayer mixtures prior to publication. This research is supported with grants from the National Science Foundation through its low-temperature physics program, DMR 8601848.

[1] J. P. Romagnan, J. P. Laheurte, J. C. Noiray, and W. F. Saam, J. Low Temp. Phys. **30**, 425 (1978); M. Chester, J. P. Laheurte, and J. P. Romagnan, Phys. Rev. B **14**, 2812 (1976); J. P. Laheurte, J. C. Noiray, and J. P. Romagnan, *ibid.* **22**, 4307 (1980).

[2] M. J. DiPirro and F. M. Gasparini, Phys. Rev. Lett. **44**, 269 (1980).

[3] F. M. Ellis, R. B. Hallock, M. D. Miller, and R. A. Guyer, Phys. Rev. Lett. **46**, 1461 (1981); F. M. Ellis and R. B. Hallock, Phys. Rev. B **29**, 497 (1984).

[4] D. McQueeney, G. Agnolet, and J. D. Reppy, Phys. Rev. Lett. **52**, 1325 (1984).

[5] B. K. Bhattacharyya, M. J. DiPirro, and F. M. Gasparini, Phys. Rev. B **30**, 5029 (1984).

[6] J. M. Valles, Jr., R. H. Higley, B. R. Johnson, and R. B. Hallock, Phys. Rev. Lett. **60**, 428 (1988).

[7] B. K. Bhattacharyya and F. M. Gasparini, Phys. Rev. Lett. **49**, 919 (1982); Phys. Rev. B **31**, 2719 (1985).

[8] J. C. Noiray, D. Sornette, J. P. Romagnan, and J. P. Laheurte, Phys. Rev. Lett. **53**, 2421 (1984); J. P. Laheurte, J. C. Noiray, J. P. Romagnan, and D. Sornette, J. Phys. (Paris) **47**, 39 (1986).

[9] E. Webster, G. Webster, and M. Chester, Phys. Rev. Lett. **42**, 243 (1979).

[10] J. P. Laheurte, J. C. Noiray, and J. P. Romagnan, see Ref. 1.

[11] E. N. Smith, D. J. Bishop, J. E. Berthold, and J. D. Reppy, J. Phys. (Paris) **39**, C6-342 (1978).

[12] F. M. Gasparini and S. Mhlanga, Phys. Rev. B **32**, 5066 (1986).

[13] The observation that superfluidity in unsaturated films exists for films thicker than one to two statistical layers goes back to E. A. Long and L. Meyer, Phys. Rev. **79**, 1031 (1950); R. Brewer, D. F. Bower, and K. Mendelssohn, Proc. R. Soc. London, Ser. A **63**, 1318 (1950). For a recent review see D. F. Brewer, in *The Physics of Liquid and Solid Helium, Part II*, edited by K. H. Bennemann and J. B. Ketterson (Wiley, New York, 1978).

[14] D. C. Hickernell, E. O. McLean, and O. E. Vilches, J. Low

Temp. Phys. **23**(1&2), 143 (1976).
[15]J. L. Cardy and D. J. Scalapino, Phys. Rev. B **19**, 1428 (1979).
[16]A. N. Berker and D. R. Nelson, Phys. Rev. B **19**, 2488 (1979).
[17]M. D. Miller, Phys. Rev. B **17**, 1139 (1978).
[18]F. M. Gasparini, B. K. Bhattacharyya, and M. J. DiPirro, Phys. Rev. B **29**, 4921 (1984).
[19](a) D. S. Sherrill and D. O. Edwards, Phys. Rev. B **31**, 1338 (1985); (b) E. Krotscheck, M. Saarela, and J. L. Epstein, Phys. Rev. B **38**, 111 (1988).
[20]See, for instance, T. Ando, A. B. Fowler, and F. Stern, Rev. Mod. Phys. **54**, 437 (1982).
[21]A. F. Andreev, Zh. Eksp. Teor. Fiz. **50**, 1414 (1966) [Sov. Phys.—JETP **23**, 939 (1966)].
[22]M. J. DiPirro, Ph.D. thesis, State Univeristy of New York at Buffalo, 1979.
[23]M. Chester *et al.*, Ref. 1.
[24]J. P. Romagnan, J. P. Laheurte, J. C. Noiray, and M. Papoular, Phys. Rev. B **37**, 5639 (1988).
[25]D. J. Bishop and J. D. Reppy, Phys. Rev. B **22**, 5171 (1980).
[26]V. R. Pandharipande and Naoki Itoh, Phys. Rev. **48**, 2564 (1973).
[27]E. L. Andronikashviili, Zh. Eksp. Teor. Fiz. **16**, 780 (1946).
[28]See, for instance, L. D. Landau and E. M. Lifshitz, *Fluid Mechanics* (Pergamon, London, 1959).
[29]G. Agnolet, Ph.D. thesis, Cornell University, 1983.
[30]We are grateful to R. J. Theis of E. I. DuPont De Nemours and Co. for providing us with the Mylar ribbon used in this experiment.
[31]See D. M. Young and A. D. Crowell, *Physical Adsorption of Gases* (Butterworth's, London, 1962).
[32]B. K. Bhattacharyya, Ph.D. thesis, State University of New York at Buffalo, 1983.
[33]R. N. Kleiman, G. K. Kaminsky, J. D. Reppy, R. Pindak, and D. J. Bishop, Rev. Sci. Instrum. **56**, 2088 (1985).
[34]X. W. Wang and F. M. Gasparini, Phys. Rev. B **34**, 4916 (1986).
[35]G. Agnolet, D. McQueeney, and J. D. Reppy, in *Proceedings of the 17th International Conference on Low Temperature Physics, LT-17,* edited by V. Eckern, A. Schmid, N. Weber, and H. Wühl (North-Holland, Amsterdam, 1984); and (private communications).
[36]K. K Mon and W. F. Saam, Phys. Rev. B **23**, 5824 (1980).
[37]X. W. Wang, Ph.D. thesis, State University of New York at Buffalo, 1987. See also X. W. Wang and F. M. Gasparini, Can. J. Phys. **65**, 1554 (1987).
[38]D. R. Nelson and J. M. Kosterlitz, Phys. Rev. Lett. **39**, 1201 (1977).
[39]This equation is only appropriate for surfaces separated by distances much greater than δ. If this were not the case in our situation, then the surface area we would obtain in our analysis would be somewhat different. This would not invalidate our analysis.
[40]W. E. Keller, Phys. Rev. **105**, 41 (1957).
[41]X. W. Wang and F. M. Gasparini, Jpn. J. Appl. Phys. **26**, 261 Suppl. 26-3 (1987).
[42]For a review of dilute mixtures of ^{3}He in ^{4}He see C. Ebner and D. O. Edwards, Phys. Rep. C **2**, 77 (1971).
[43]D. S. Greywall, Phys. Rev. B **20**, 2643 (1979).
[44]Recent NMR measurements do not see this tranistion, see Ref. 6.
[45]For $1/D=0$ we have used $m=1.45\pm0.1$. See D. O. Edwards and W. Saam in *Progress in Low Temperature Physics,* edited by D. F. Brewer (North-Holland, Amsterdam, 1978), Vol. VIIa, p. 283.
[46]R. A. Guyer and M. D. Miller, Phys. Rev. B **22**, 142 (1980).
[47]R. A. Guyer, Phys. Rev. Lett. **53**, 795 (1984).
[48]J. L. Epstein and E. Krotscheck, Phys. Rev. B **37**, 1666 (1988).
[49]M. A. Paalanen and Y. Iye, Phys. Rev. Lett. **44**, 333 (1985); D. Cieslikowski, A. J. Dahm, and P. Leiderer, Phys. Rev. Lett. **58**, 1751 (1987).
[50]J. D. Maynard and M. H. W. Chan, Physica **109&110B**, 2090 (1982).